Expression of Sonic Hedgehog (SHH) in Human Lung Cancer and the Impact of *YangZheng XiaoJi* on SHH-mediated Biological Function of Lung Cancer Cells and Tumor Growth

WEN G. JIANG[1], LIN YE[1], FIONA RUGE[1], PING-HUI SUN[1], ANDREW J. SANDERS[1], KI JI[1], JANE LANE[1], LIJIAN ZHANG[2], LUCY SATHERLEY[1], HOI P. WEEKS[1], XIUYI ZHI[3], YONG GAO[4], CONG WEI[4], YILING WU[4] and MALCOLM D. MASON[1]

[1]*Cardiff University-Peking University Cancer Institute, Cardiff University School of Medicine, Cardiff, UK;*
[2]*Department of Thoracic Surgery, Peking University Cancer Hospital, Haidian, Beijing, P.R. China;*
[3]*Cancer Institute of Capital Medical University and Department of Thoracic Surgery, XuanWu Hospital, Capital Medical University, Beijing, P.R. China;*
[4]*Yiling Medical Research Institute, Shijiazhuang, Hebei Province, P.R. China*

Abstract. *Sonic Hedgehog (SHH) is a protein that is aberrantly expressed in various human tumors. SHH and its signaling molecules have been indicated as potential therapeutic targets. In the present study, we evaluated the expression of SHH transcript in human non-small cell lung cancer (NSCLC) tissues and investigated the impact of inhibiting SHH together with a traditional Chinese medicine formula, YangZheng XiaoJi (YZXJ), on the function and growth of lung cancer cells. Human NSCLC tissues had significantly higher levels of the SHH transcript compared matched normal lung tissues (n=83). TNM2 tumors and tumors with pleural invasion had higher levels than TNM1 and non-invasive tumors. High SHH levels were associated with a shorter overall survival (OS) of the patients. A SHH inhibitor, cyclopamine, and YZXJ alone or in combination had a marked inhibitory effect on cellular invasion and cellular migration of human lung cancer cells, A549 and SKMES1. YangZheng XiaoJi and its combination with cyclopamine also significantly reduced the growth of lung tumors in vivo together with a reduction of SHH and smoothened (Smo) proteins in the lung tumors. The present study provides evidence that blocking SHH by way of small inhibitor and by YangZheng XiaoJi has a profound influence on lung cancer cells as seen by in vitro invasion and cell migration and in vivo tumor growth. Together with the aberrant expression of SHH in NSCLC tumors in the patients, it is suggested that SHH is a potential target for therapies for NSCLC.*

Correspondence to: Wen G. Jiang, Cardiff University-Peking University Cancer Institute, Cardiff University School of Medicine, Henry Wellcome Building, Heath Park, Cardiff CF14 4XN, U.K. Tel: +44 2920687065, e-mail: jiangw@cf.ac.uk

Key Words: Sonic hedgehog (SHH), lung cancer, tumor model, *YangZheng XiaoJi*, cellular migration, invasion, cyclopamine, Smo, Gli.

Sonic Hedgehog (SHH), a mammalian homologue of the Hedgehog (HH), is a lipid modified protein that, *via* specific signaling pathways, regulates a range of physiological (such as development and tissue regeneration) and pathological (such as cancer and rheumatism) events. After synthesis within the cells, it undergoes autocatalytic cleavage and lipid modification before secretion into the extracellular space. On the target cells, SHH interacts with and activates its receptor, a 12-pass transmembrane protein Patched (Ptch). Activation of the Patched results in its de-coupling from another transmembrane protein, Smoothened (Smo), which has 7-transmembrane passes and its functions are inhibited by the non-activated Patched protein (1-5). De-coupled Smo from Patched enables Smo to form a cytosolic protein complex with G-protein receptor proteins and activates downstream proteins including SuFu and transcription factor Gli. Activated Gli then translocates to the nucleus and activates other downstream targets including Wnt, SNA1 and certain ATPases (6-8). This results in transcription activation of a number of genes that are essential for cell and body to function.

The role of SHH and its associated signaling proteins, as well as pathways in cancer, have been explored over the past decade. Its aberrant expression has been reported in a broad range of human cancer types. In retinoblastoma and glioblastoma, SHH was found to be frequently expressed and associated with disease progression (9-12). Medulloblastoma

is another tumor type strongly associated with the SHH pathway (11-13). In breast cancer, expression of proteins related to SHH is linked to a poor survival (14). In prostate cancer, SHH has been shown to be activated, possibly by the loss of SuFu, and indicated as a possible factor in driving the metastasis and progression of the cancer (15). Other studies have also indicated SHH as a target for therapy in prostate cancer (16, 17). In gastric cancer, SHH and Patched are linked to a poor outcome of the patients and its activation has been linked to *H. Pylori* (18-20). The therapeutic value by targeting SHH in pancreatic cancer is strongly indicated (21-24). The same therapeutic value has also been indicated in clear cell renal cancer (25). These data indicate that the SHH pathway is a promising target in cancer therapies. The past few years have witnessed the discovery and development of a number of therapeutic tools in targeting the pathway with some being currently in late stage clinical trials. The well documented inhibitor to SHH is cyclopamine, a naturally occurring small compound shown to be highly effective in blocking the SHH pathways. Other compounds, including GDC0449 (for skin, colorectal and brain cancers) (26), LDE-225 (for breast cancer), BMS-833923, PF-0449913 (for leukaemia), from the industry are now in early to late clinical trials (27-31).

The role for SHH in the development and pathology of the lungs has been indicated in recent years. In human lung cancer, however, its role remains controversial (32). A study using tissue array (n=248) has shown that SHH staining was correlated with that of Smo, Gli-1 and Gli-2 but did not have correlations with clinical and pathological features of the lung cancer tissues (33). In a study based on immunohistochemical analyses on 81 NSCLC tumors, it has been shown that the staining for SHH, Gli and Smo were weak and that staining for Patched was almost negative. In another immunohistochemically- based study with 40 NSCLC tissues, Hwang *et al*. (35) has shown that SHH and a specific lymphangiongenic marker, LYVE-1, were significantly correlated with pleural invasion and lymphatic thromboembolism. This study has reported that SHH expression levels were significantly correlated with a shorter survival ($p<0.05$). However, another study that employed a similar method has delivered an opposite observation in that high expression was said to be related to a better survival of the patients (36). It has been shown that smoking-induced lung cancers may be the result of activation of SHH and Wnt (37). In another study, which examined SHH, Gli, Patched, Smo protein expression in NSCLC, all the proteins were found over-expressed in NSCLC compared to their adjacent non-neoplastic lung parenchyma. The study reported that SHH and Patched are associated with node metastasis and that their levels were high in squamous cell carcinoma of the lungs (38).

Recently, we reported that a traditional Chinese medicine formula, *YangZheng XiaoJi*, which has been used in treating patients with liver and lung cancer (39, 40), is able to inhibit the angiogenic status and migration of cancer cells, including lung cancer cells. The medicine has been found to enhance the efficacy of chemotherapy in liver and lung cancers and reduce the side-effects from the traditional therapies (39, 40). We further demonstrated that the medicine appears to inhibit with intracellular signalling events, including the focal adhesion kinase (FAK) pathway, in both endothelial and cancer cells and the AKT pathway in cancer cells (41, 42) suggesting that the medicine, formulated with 16 herbs, has a tendency to interact with the signaling events. In a screen exercise, in order to identify the key signaling events affected by the medicine, we found that SHH was one such pathway that had response to *YangZheng XiaoJi*. Herein, we investigated the gene transcript expression pattern of SHH in a cohort of human non-small cell lung cancer and then tested the response of lung cancer cells to *YangZheng XiaoJi in vitro* and *in vivo*.

Materials and Methods

Materials. A SHH inhibitor, cyclopamine, and a negative control compound, tomatidine, were obtained from Tocris Chemicals (Bristol, England, UK). Antibodies to human SHH, Patched, Gli and Smo were obtained from Santa Cruz Biotechnologies Inc., (Santa Cruz, CA, USA). Fluorescent tagged secondary antibodies were obtained from Sigma Aldrich (Poole, Dorset, England, UK). *YangZheng XiaoJi* extract, referred to as *YZXJ* (*DME25*), was prepared from *YangZheng XiaoJi* as we previously reported (41-43). Matrigel was obtained from Laboratory Scientific Suppliers (Hessle, East Riding, Yorkshire, England, UK).

Lung cancer tissues and cell lines. Paired fresh-frozen non-small cell lung cancer (NSCLC) carcinoma tissues at TNM stages of I to III and matched normal tissues were obtained from 83 patients who received a curative resection in Peking University Cancer Hospital from January 2003 to December 2011. Ethical approval was provided by the Peking University Cancer Hospital Ethics Committee. Clinical and pathological information of the patients is given in Table I. These tissues were collected immediately after surgical resection and stored in the Tissue Bank of Peking University Cancer Hospital. Clinical and pathological information, including age, sex, smoking history, histological types of tumors, TNM stage and lymph node metastasis, were collected and stored in the patients' database. Patients were followed up from the day of surgical operation to December 2009. The follow-up intervals were calculated as survival intervals after surgery. Human lung squamous carcinoma SKMES1 and human lung adenocarcinoma A549 cells were obtained from LGC Standard/ATCC (American Type Culture Collection) (Teddington, Middlesex, England, UK). Cells were routinely cultured with Dulbecco's modified Eagle's medium (DMEM) F12 supplemented with 10% foetal calf serum, penicillin and streptomycin (Sigma Aldrich).

RNA isolation and quantitative reverse transcription polymerase chain reaction (QPCR). Total RNA was isolated from the homogenized NSCLC and normal lung tissues and cell lines using a Triagent total RNA isolation reagent (Sigma Aldrich). Reverse transcription was performed using the Reverse Transcription kit

Table I. *SHH transcript expression and clinical/pathological characteristics of lung cancer.*

Clinical/pathological features	Mean±SD	*p*-Value
Total cohort (n=83 pairs)		
Paired tumor tissue	16.5±15.0	0.01
Paired background tissue	9.7±9.2	
Histology		
Squamous carcinoma	1.9±1.4	
Adenocarcinoma	31.9±30.0	0.16
Other	0.6±0.3	N.A.
TNM staging		
I	0.18±0.12	
II	28.4±26.0	0.03
III	1.5±0.09	0.17
Tumor differentiation		
High	0.001±0.01	
Medium/High	37.5±36.1	0.19
Low/Medium	0.3±0.02	0.32
Lymph node status		
Node negative	1. 8±1.5	0.30
Node positive	34.5±30.2	
Pleural invasion		
No	0.46±0.3	0.033
Yes	90.8±88.6	
Smoking status		
Former or current smoker	4.5±2.5	
Non smoker	21.6±20.3	0.043

(Primer design). QPCR was performed on the Icycler IQ5 system (Bio-Rad, Hammel Hemstead, UK) to quantify the level of *SHH* transcripts in the NSCLC specimens (shown as copies/l from internal standard). NSCLC cDNA samples were then examined for *SHH* transcript expression, along with a set of standards and negative controls. The QPCR technique utilised the Amplifluor system™ (Intergen Inc., City, England) and QPCR master mix (BioRad). Pairs of primers were designed using the Beacon Design software (PREMIER Biosoft, Palo Alto, CA, USA): The housekeeping control was *GAPDH* (Glyceraldehyde-3-phosphate dehydrogenase) primers (sense: 5'-ctgagtacgtcgtggagtc-3'; antisense: 5' actgaacctgaccgtacacagagatgatgaccctttg -3') and *SHH* mRNA levels were assessed using *SHH* specific primers as follow: 5'-caaccccgacatcatattta -3' and 5'-actgaacctgaccgtacaactggttcat caccgaga-'. The underlined sequence in the reverse primers was the additional Z sequence, which is complementary to the universal Z probe (TCS Biologicals Ltd., Oxford, UK). Real-time QPCR conditions were 95˚C for 15 min, followed by 60 cycles of 95˚C for 20 s, 55˚C for 30 s and 72˚C for 20 s.

Scratching wounding assay using the EVOS cellular migration system. Cells were seeded into a 96-well plate (Nunc, Fisher Scientific, Paisley, Scotland, UK) at 10,000 per well and allowed overnight in the incubator to reach full confluence. The monolayer was then scratched using a fine-tipped plastic pipette to create a wound of approximate 200 μm. The media, together with the floating cells, were removed and replaced with media together with *YangZheng XiaoJi* extract alone, cyclopamine alone, tomatidine alone or in combination with *YangZheng XiaoJi*. The plate was immediately placed in the chamber of the EVOS unit (EVOS^{tm} fl Digital Inverted Fluoresceince Microscope; Fisher Scientific), which was programmed to supply 5% CO_2 and maintained at 37˚C constant temperature. The EVOS was then programmed to memorise the three dimensional position of the wounding position in each well and then automatically tracked the image of each well, every 15 minutes for up to 9 hours. Sequential images were analysed using the Image J software. The net distance that the cell migrated was calculated as: distance migrated=(T0-Tn)/2, in which T0 is the distance between two leading wound edges at the beginning of the experiment, Tn is the distance between the wound leading edge of the same wounding point at a given time. The distance is shown here as the number of pixels that cells had migrated. The migration is shown as a time course and the comparison between the experimental settings was based on a fix time point.

Electric cell-substrate impedance sensing (ECIS)-based cellular migration assays. This was modified from a method previously described (44, 45). Briefly, 96-well 96W1E microarrays, which have a gold-plated electrode at the bottom of each well, were used on the ECIS Ztheta instrument (Applied Biophysics Ltd, Troy, NJ, USA). Lung cancer cells were added to the wells of the array, followed by immediate tracking of cell adhesion over a range of frequencies, namely from 1,000 Hz to 64,000 Hz, using an automated modules. Once the cells reached confluence, the electric wounding module was activated and applied a current of 2,000 mA for 20 sec for each well (35). The migration of the cells was immediately tracked after wounding, again over a range of frequencies. All the experiments were conducted in triplicate. Cell migration was analysed using the two dimensional and three dimensional models.

In vitro invasion assay. This was based on a matrigel transwell invasion model previously published (46). Transwell invasion insert (Greiner Bio., Gloucester, UK) with pore size at 8.0 μm was first coated with 50 μg Matrigel and allowed to air dry. The gel was then carefully rehydrated. To each insert, 30,000 cancer cells were added together with the test agents or their combinations. After 72 h, Matrigel and non-invading cells were removed using a cotton swab. The invaded cells on the lower surface of the inserts were fixed with 4% formaldehyde and then stained with 1% crystal violet. The number of invaded cells was counted under a microscope.

In vivo tumor model. Athymic female nude mice, CD-1 of 4-6 weeks old were purchased from Charles River Laboratories (Margate, Kent, UK). A549 tumor cells, which were prepared at 5×10^6/ml in a solution containing 3mg/ml Matrigel, were injected subcutaneously to give 0.5 million cells per injection (47). After one week, when tumors became visible, mice were randomly divided into groups (n=6 in each group). The size of tumors was measured using a digital caliper. Treatments began one week after tumor cell inoculation and included the following: Control group (receiving control buffer), *YangZheng XiaoJi* extract *via* intraperitoneal injection (IP) or by gavage (oral), cyclopamine, a combination of *YangZheng XiaoJi* extract and cyclopamine. Treatments were given daily. The final concentration for *YangZheng XiaoJi* extract was 1:1,000 and cyclopamine. Mice were weighed and monitored daily. Tumour size was measured weekly for 4 weeks. The procedure was reviewed and approved by the Cardiff University Joint Biological Ethics Committee and conducted under the UK Home Office Project

License (PPL 30/2591). At the conclusion of the experiments, mice were terminated by euthanasia. Tumours were dissected and immediately stored at –80˚C for subsequent immunohistochemical analyses. The volume of tumors was calculated by the following formula: tumor volume (mm^3)=length × width × 0.54 (48).

Immunofluorescence staining. Frozen tumors were sectioned using a cryostat (Leica DMR, Bristol, UK) at 10 μm thickness. After fixation, using acetone/methanol fixation buffer, the slides were rehydrated and blocked with a Tris buffer (25 mM, pH 8.4) that contained 10% horse serum for one hour. Primary antibodies (including anti-SHH, anti-Gli, anti-Ptch and anti-Smo), diluted in the blocking buffer, were added to the respective slides that were kept in dark in full humidity on a slow moving platform for one hour and then thoroughly washed. FITC-tagged secondary antibodies were then added to the respective slides together with DAPI for nucleus counter stain. After one hour, the slides were thoroughly washed and mounted using FluoSave™ (Calbiochem, Nottingham, UK). The slides were examined on an Olympus microscope (London, UK) and photographed using a Hamamatsu digital camera (Hertfordshire, UK).

Statistical analysis. This was carried out using SigmaPlot (Version 11; Systat Software Inc., San Jose, CA, USA). The Student's *t*-test and one way analysis of variance (ANOVA) were used where appropriate.

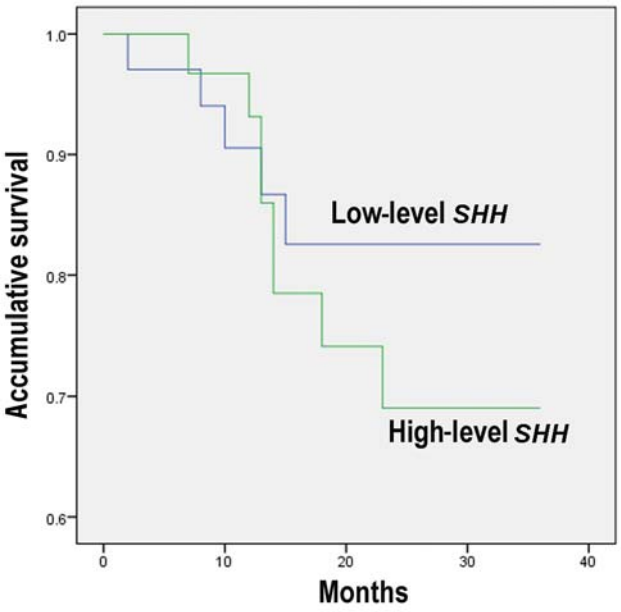

Figure 1. *Levels of the SHH transcript and the overall survival of the patients with NSCLC. Patients with high levels of SHH transcript had a shorter survival, although this yet to reach statistical significance (p>0.05).*

Results

SHH expression in NSCLC. We first evaluated the *SHH* transcript levels in a cohort of paired lung tissues from patients with NSCLC. As shown in Table I, lung tumor tissues expressed high levels of *SHH* transcript (p=0.01) compared to matched normal lung tissues. Both TNM-2 and TNM-3 tumors showed high levels of the transcript when compared with TNM-1 tumors, although only TNM-2 showed a statistical difference (p=0.01, *vs*. TNM-1). It is interesting to note that tumors with pleural invasion and tumors from patients with smoking history had high levels of *SHH* transcript than that from the respective non-pleural invasion and non-smoking patients. There are no significant correlations between SHH, histological types and the degree of differentiation of the NSCLC tumors. Patients with high levels of *SHH* transcript tends to have shorter survival, although this is not statistically significant (p>0.05) (Figure 1).

YZXJ and cycloplamine had marked effects on cellular migration. We employed two independent methods for assessing the migration of cancer cells, namely a scratch wounding-based assay using an EVOS automated tracking system and an electric cell-substrate sensing (ECIS) method both of which provided a human interface-free and automated monitoring of cell migration. Figure 2 shows representative images from A549 cells (top panel: immediately after scratching; Bottom panel: 5 hours after scratching). Over the indicated time period, wounding space in control cells almost closed (Figure 2, left). *YangZheng XiaoJi* treatment and indeed cyclopamine reduced the pace of cell migration. The combination of both *YangZheng XiaoJi* and cyclopamine reduced the migration (Figure 2, right). Quantitative analyses of cellular migration are shown in Table II in which *YangZheng XiaoJi* and cyclopamine exhibit a significant inhibitory effect on the migration, while the combination of both results in a more profound reduction. It is interesting to note that a control chemical, tomatidine, which has similar chemical structure to cyclopamine but does not interact with SHH, showed little effect on the cellular migration (Table II).

Using the ECIS-based method, similar inhibitory effects by *YangZheng XiaoJi* and cyclopamine and their combinations were observed (Figure 3). Over a broad range of frequencies tested, the inhibitory effects were largely consistent (Figure 4).

Cell invasion was also reduced by YangZheng XiaoJi and cycloplamine affected cellular invasion. We employed a Matrigel-based method to assess the *in vitro* invasiveness of both cancer cells. As shown in Table II, *YangZheng XiaoJi* and cyclopamine-alone exhibited significant inhibitory effects on the invasion of both lung cancer cells. The combination of *YangZheng XiaoJi* and cyclopamine showed a more profound inhibitory effect than each individual agent when used alone (Table II).

The impact of YangZheng XiaoJi and cycloplamine and tumor growth. To further evaluate the effect of *YangZheng XiaoJi*

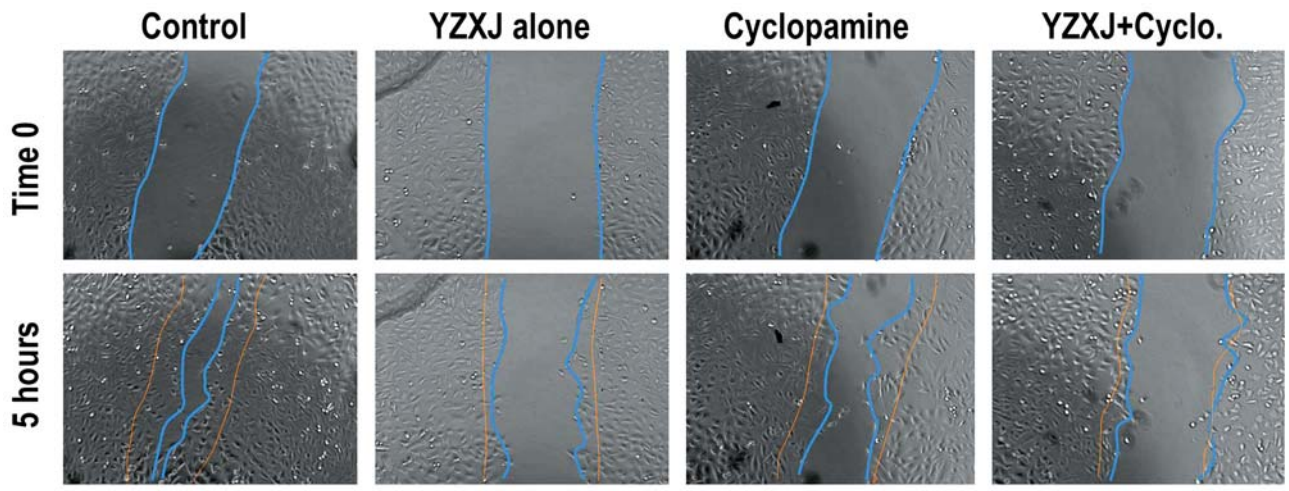

Figure 2. *Effect of YangZheng XiaoJi and cyclopamine on the migration of A549 cells. Cells were seeded in a 96-well plate. On reaching confluence, they were scratch-wounded and then immediately and continuously recorded on a EVOS cell imaging system over a 5-h period. Shown here are images of A549 cells immediately after wounding (top panel) and 5 hours after wounding (bottom panel). From Left to Right are: control cells (treated with culture medium only); cells treated with YangZheng XiaoJi ; cells treated with cyclopamine and cells treated with the combination of YangZheng XiaoJi and cyclopamine. Blue lines indicate the leading front of the cells at the time point specified. Light yellow lines in the bottom panel indicate the initial position of the leading front following wounding.*

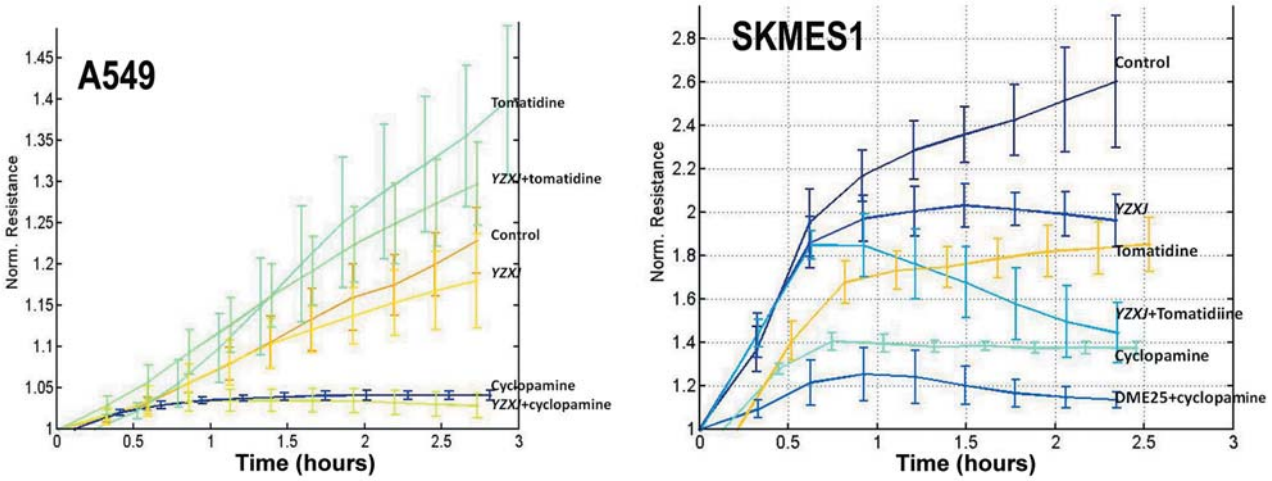

Figure 3. *Cell migration assessed by electric cell-substrate impedance sensing (ECIS). Upon reading confluence within the 96W1E ECIS arrays, cells (Left: A549 cells; Right: SKMES1 cells) were electrically wounded and their electrical resistance recorded immediately after wounding. The respective treatment of the cells is indicated in the figure.*

and cyclopamine on cancer cells, an *in vivo* tumor model was used in which A549 cells were subcutaneously injected together with Matrigel. When tumor became visible and measurable after one week, the treatment began by delivering the agents *via* intra-peritoneal injections. As shown in Figure 5, after two weeks of treatment, *YangZheng XiaoJi* had a significant effect on the growth of tumors, so as the *YangZheng XiaoJi*/cyclopamine combination. Although cyclopamine demonstrated some degree of inhibitory effect, at the concentration used in the present study, this effect was not statistically significant (Figure 5).

SHH and its signaling molecules in response to YangZheng XiaoJi and cyclopamine. We examined the protein expression of SHH, Ptch, Gli and Smo in lung tumors by immunofluorescence staining of the specific proteins. It was

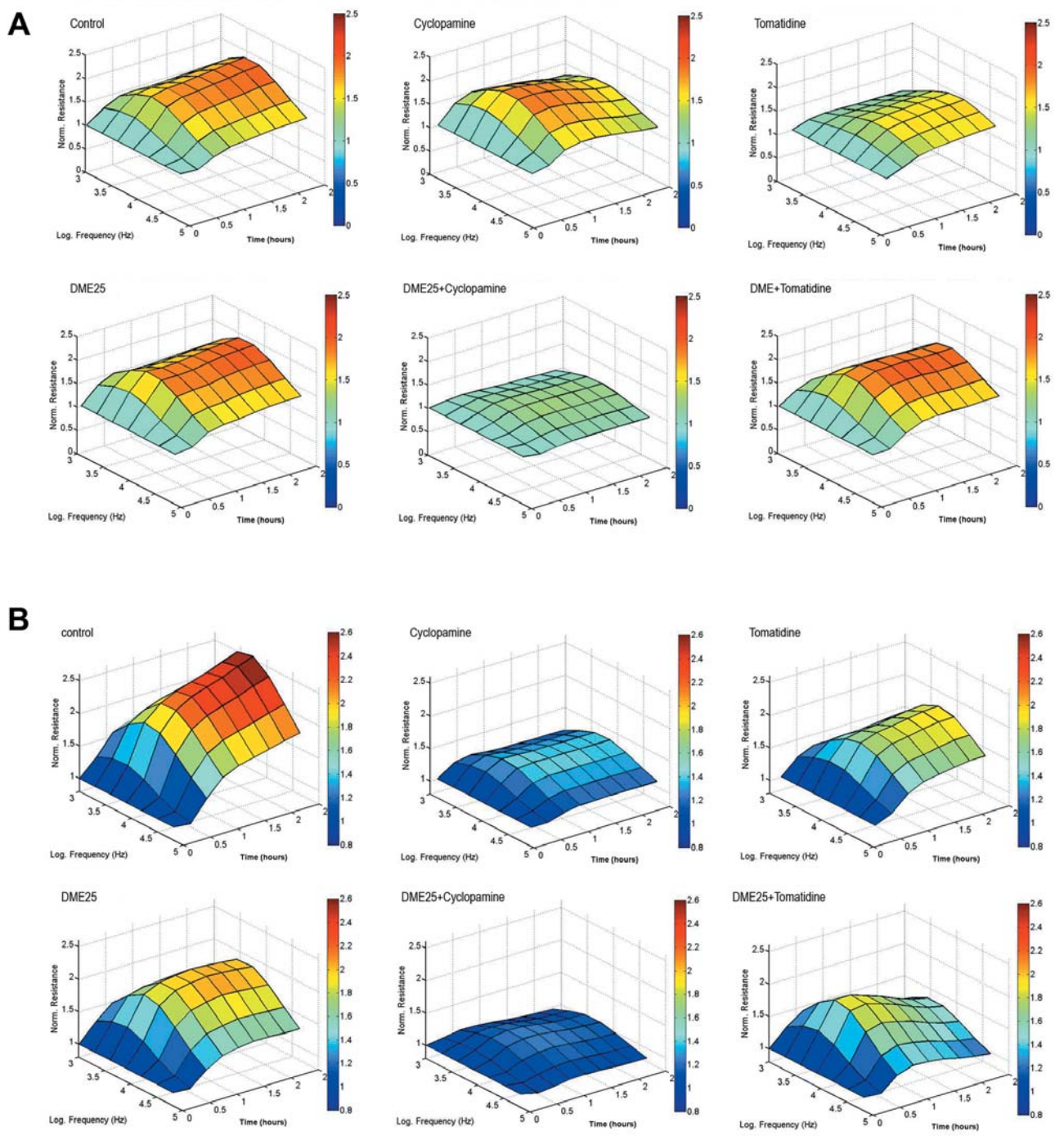

Figure 4. *Cell migration assessed by electric cell-substrate impedance sensing (ECIS) and migration demonstrated in a three dimensional graph. The experimental conditions are the same as in Figure 3, except that the responses of the cells are displayed over a three dimensions, namely y-axis for electrical resistance, x-axis for frequencies (shown in Hz) and z-axis for time (in hours). A: A549 cells, B: SKMES1 cells.*

found that out of all proteins evaluated, SHH had the most demonstrable change in which *YangZheng XiaoJi*, but not cyclopamine, reduced staining of the protein (Figure 6A). The combination of *YangZheng XiaoJi* and cyclopamine resulted in almost complete loss of the staining. Reductions of Smo were also seen under both *YangZheng XiaoJi* and cyclopamine (Figure 6C). There were no marked changes in the staining for Gli and Patched (Figure 6B and D).

Table II. *Effects of YZXJ and SHH inhibitors on cellular migration and invasion and migration of lung cancer cells, A549 and SKMES1.*

	Control	YZXJ	Cyclopamine	Cyclopamine plus YZXJ	Tomatidine	Tomatidine plusYZXJ
Migration[c]						
A549	209.6±32.5	143.2±45.4[a]	150.8±32.4[a]	60.5±21.8[a,b]	192.4±28.6	125.8±33.2[a,b]
SKMES1	204.3±42.7	134.0±20.6[a]	149.7±42.0[a]	102.5±25.9[a]	187.5±45.2	130.0±40.5[a,b]
Invasion[d]						
A549	41.2±7.8	25.8±3.0[a]	30.0±7.6[a]	24.0±5.1[a,b]	38.7±4.6	39.3±5.2
SKMES1	38.8±3.5	31.0±3.4[a]	25.0±4.9[a]	22.5±4.0[a,b]	36.5±2.6	33.8±5.3[a]

[a]$p<0.05$ *vs*. control; [b]$p<0.05$ *vs*. YZXJ alone. [c]Migration: shown are pixels that cell migrated in the scratch wounding assay. [d]Invasion: shown are the number of cancer cells invaded through the matrix protein layer.

Discussion

The SHH and its pathways have been implicated as potential therapeutic targets in a number of solid human tumors including neurological, gastrointestinal, pancreatic, breast and prostate cancers in which SHH and its associated signalling molecules are aberrantly expressed and linked to disease progression and prognosis. In lung cancer, the link is far from clear, with some studies showing that it is highly expressed and some showing the opposite. The present study has shown that at transcript level, SHH is significantly raised in non-small cell lung cancer tissues compared with normal tissues. This is in line with previous findings using immunohistochemical methods (33, 35, 37) but in contrast to others in which SHH expression was reported to be a favourable factor for disease progression (36). The controversies in the expression in lung cancer can also be explained by the methods applied and the fact that its activation and expression differ markedly *in vivo* and *in vitro* (49) and that the activation is more likely to exist in a subset of lung cancers (50) and as indicated in early studies (51).

In the present study, we provided compelling evidence to indicate that by blocking the SHH pathway using a SHH inhibitor, cyclopamine, it is possible to markedly reduce cellular migration and invasion *in vitro* suggesting that blocking SHH is indeed a useful approach in combating the aggressive behaviour of lung cancer cells. The findings from *in vivo* tumor models further demonstrate that the SHH pathway is a very useful target in lung cancer therapies.

A major goal of the present study was to investigate if *YangZheng XiaoJi* is a useful adjunct to anti-SHH treatment. Clinically, *YangZheng XiaoJi* has been reported to be beneficial to patients with liver and lung cancers when used alone or in combination with chemotherapy (39, 40). In our recent work, we reported that *YangZheng XiaoJi* can interplay with the FAK and AKT pathways by suppressing the activation of these kinases (41,42). SHH was an alternative signal pathway identified from our screening on the action of *YangZheng XiaoJi*. Herein, we showed that

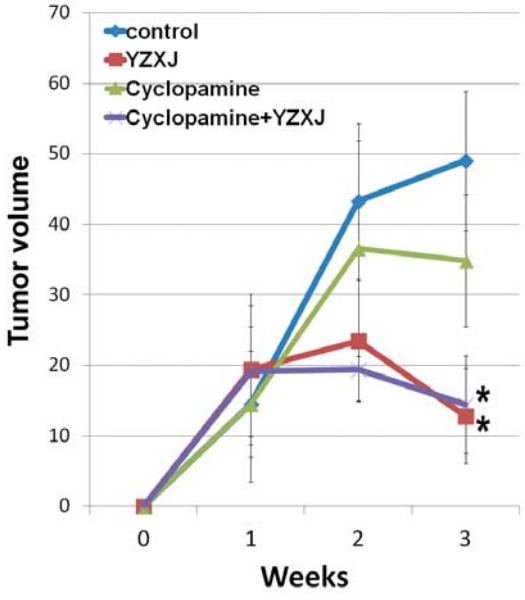

Figure 5. *Effect of YangZheng XiaoJi, cyclopamine and their combination on the in vivo growth of A549 tumors. Cancer cells were subcutaneously injected (week 0). Treatment (via intra-peritoneal injection) began after one week and was given daily. Shown are tumor volumes in mm^3. *p<0.05 vs. control group by one way ANOVA.*

YangZheng XiaoJi was able to reduce the amount of SHH in lung cancer tissues as seen in our *in vivo* tumor models.

Another highlight of the present study is the finding that *YangZheng XiaoJi* can potentiate the action of cyclopamine on cancer cell, including increased inhibition of cell invasion and cellular migration *in vitro* and tumor growth *in vivo*. This is interesting as it has been suggested that the SHH pathway, in particular Gli1, is a mechanism in inducing drug resistance (52, 53). It is possible, therefore, that the combined use of the SHH inhibitor and *YangZheng XiaoJi* may assist in overcoming drug resistance, an interesting lead for future studies. Second, in lung cancer, the SHH pathway has been shown to cross-talk with other pathways including the

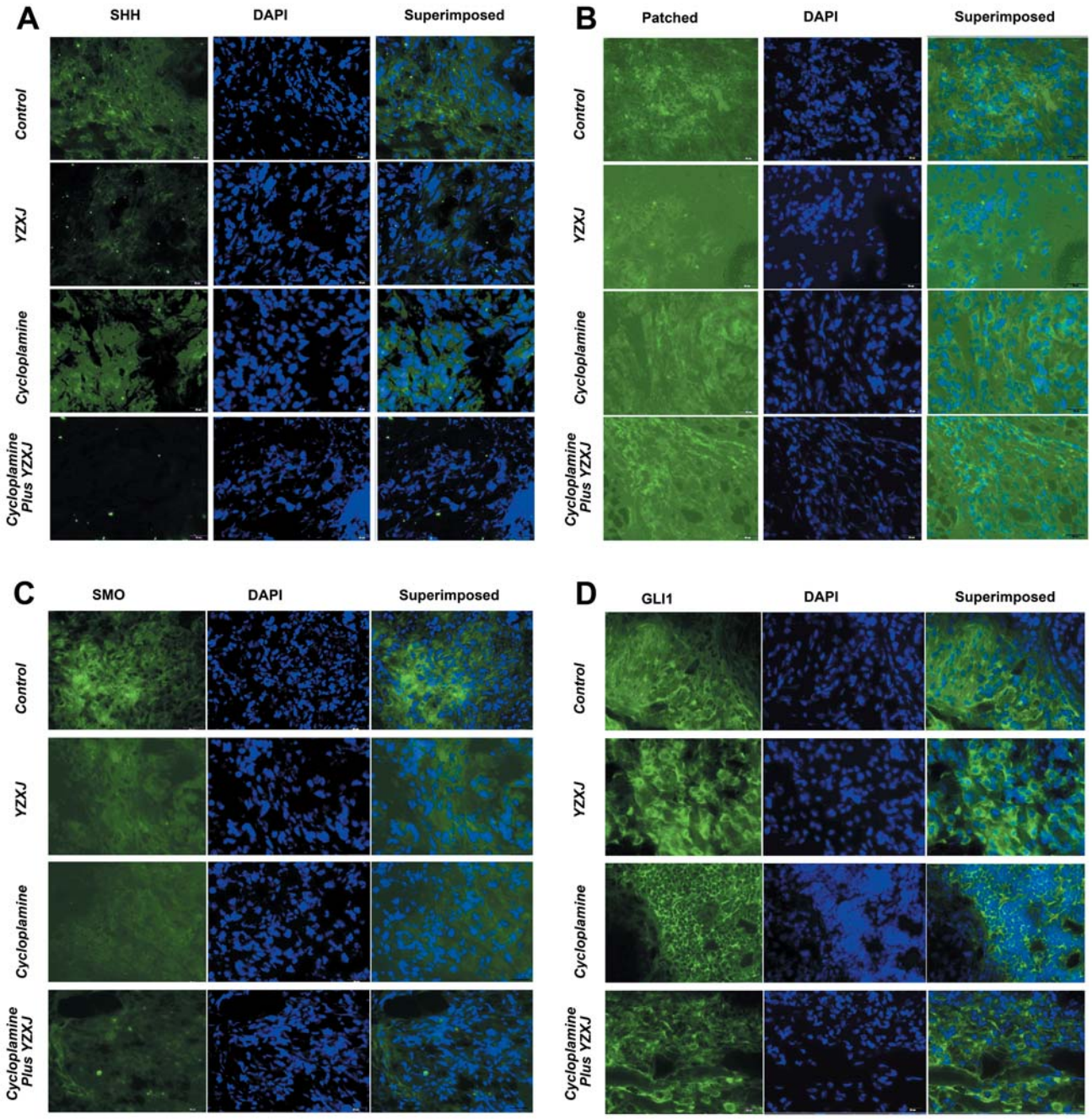

Figure 6. *Immunofluorescent staining of SHH (A), Patched (Ptch) (B), Smo (C) and Gli (D) in lung tumor tissues from the in vivo tumor model. The specific protein staining is seen in green colour (FITC tagged secondary antibody); nucleus staining in blue (DAPI) in the respective panels.*

bombesin neuropeptide receptor pathway, which provides other opportunities for combined treatment with other targeted therapies (54). The observed effects of *YangZheng XiaoJi*, namely on the cellular migration and invasion, may further indicate that it plays a role in the process of epithelial to mesenchymal transition (EMT). It has been reported that SHH up-regulation may contribute to transforming growth factor beta-induced EMT in lung cancer (55, 56) and the effects of *YangZheng XiaoJi* here again indicate the diverse effects of the medicine on cancer cells, including lung cancer cells.

YangZheng XiaoJi is made of natural herbs and is, therefore, comprised of a large number of natural products.

A number of botanical compounds have been indicated as being potential inhibitors for the SHH/Gli pathway (57). These include a broad range of well-known as less well-investigated compounds curcumin, genistein, epigallocatechin gallate, resveratrol, quercetin, baicalen and apigenin, along with novel compounds isolated from Southeast Asian plants, such as the potent sub-micromolar gitoxigenin derivatives. In fact, cyclopamine is also a naturally-occurring product. Thus, the natural products appear to be a rich source of anti-SHH options. Presently, it is not clear which compound or compounds in *YangZheng XiaoJi* result in the anti-SHH effects as observed in the current study, which poses a future challenge. However, given that most modern therapies, including chemotherapy, radiotherapy and targeted therapy, require a combined approach to enhance efficacy, overcome resistance and reduce side-effects, a combined approach using anti-SHH agents and *YangZheng XiaoJi* would be a useful suggestion, when devising new therapies for lung cancer.

In conclusion, SHH is aberrantly expressed in human NSCLC tissues and appears to be linked to disease progression and clinical outcome. We further demonstrated that a traditional Chinese medicine formula, *YangZheng XiaoJi*, is able to potentiate the effect of cyclopamine, an inhibitor for SHH, in the inhibition of cellular migration, invasion and tumor growth of lung cancer cells. The study, thus, suggests that *YangZheng XiaoJi* and inhibitors to SHH pathway would be a viable option in the treatment of non-small cell lung cancer and warrant future investigations.

Acknowledgements

The Authors wish to thank Cancer Research Wales, Albert Hung Foundation and Ser Cymru Welsh Life Science Fund for supporting their work.

References

1 Echelard Y, Epstein DJ, St-Jacques B, Shen L, Mohler J, McMahon JA and McMahon AP: Sonic hedgehog, a member of a family of putative signaling molecules, is implicated in the regulation of CNS polarity. Cell *75*: 1417-1430, 1993.

2 Marigo V, Roberts DJ, Lee SMK, Tsukurov O, Levi T, Gastier JM, Epstein DJ, Gilbert DJ, Copeland NG, Seidman CE, Jenkins NA, Seidman JG, McMahon AP and Tabin C: Cloning, expression, and chromosomal location of SHH and IHH: two human homologues of the Drosophila segment polarity gene hedgehog. Genomics *28*: 44-51, 1995.

3 Chen Y and Struhl G: Dual roles for Patched in sequestering and transducing hedgehog. Cell *87*: 553-563, 1996.

4 Agarwala S, Sanders TA and Ragsdale CW: Sonic hedgehog control of size and shape in midbrain pattern formation. Science *291*: 2147-2150, 2001.

5 Bale AE and Yu KP: The hedgehog pathway and basal cell carcinomas. Hum Molec Genet *10*: 757-762, 2001.

6 Quirk J, van den Heuvel M, Henrique D, Marigo V, Jones TA, Tabin C and Ingham PW: The Smoothened gene and hedgehog signal transduction in Drosophila and vertebrate development. Cold Spring Harbor Symp Quant Biol *62*: 217-226, 1997.

7 Zuniga A, Haramis APG, McMahon AP and Zeller R: Signal relay by BMP antagonism controls the SHH/FGF4 feedback loop in vertebrate limb buds. Nature *401*: 598-602, 1999.

8 Ahn S and Joyner AL: *In vivo* analysis of quiescent adult neural stem cells responding to Sonic hedgehog. Nature *437*: 894-897, 2005.

9 Xu Q, Yuan X, Liu G, Black KL and Yu JS: Hedgehog signaling regulates brain tumor-initiating cell proliferation and portends shorter survival for patients with PTEN-coexpressing glioblastomas. Stem Cells *26*: 3018-3026, 2008.

10 Choe JY, Yun JY, Jeon YK, Kim SH, Choung HK, Oh S, Park M and Kim JE: Sonic hedgehog signalling proteins are frequently expressed in retinoblastoma and are associated with aggressive clinicopathological features. J Clin Pathol 8. pii: jclinpath-2014-202434. doi: 10.1136/jclinpath-2014-202434. [Epub ahead of print], 2014, in press.

11 Brun SN, Markant SL, Esparza LA, Garcia G, Terry D, Huang JM, Pavlyukov MS, Li XN, Grant GA, Crawford JR, Levy ML, Conway EM, Smith LH, Nakano I, Berezov A, Greene MI, Wang Q and Wechsler-Reya RJ: Survivin as a therapeutic target in Sonic hedgehog-driven medulloblastoma. Oncogene. doi: 10.1038/onc.2014.304. [Epub ahead of print], 2014, in press.

12 Crawford TQ and Roelink H: The notch response inhibitor DAPT enhances neuronal differentiation in embryonic stem cell-derived embryoid bodies independently of sonic hedgehog signaling. Dev Dyn *236*: 886-892, 2007.

13 Kool M, Jones DT, Jäger N, Northcott PA, Pugh TJ, Hovestadt V, Piro RM, Esparza LA, Markant SL, Remke M, Milde T, Bourdeaut F, Ryzhova M, Sturm D, Pfaff E, Stark S, Hutter S, Seker-Cin H, Johann P, Bender S, Schmidt C, Rausch T, Shih D, Reimand J, Sieber L, Wittmann A, Linke L, Witt H, Weber UD, Zapatka M, König R, Beroukhim R, Bergthold G, van Sluis P, Volckmann R, Koster J, Versteeg R, Schmidt S, Wolf S, Lawerenz C, Bartholomae CC, von Kalle C, Unterberg A, Herold-Mende C, Hofer S, Kulozik AE, von Deimling A, Scheurlen W, Felsberg J, Reifenberger G, Hasselblatt M, Crawford JR, Grant GA, Jabado N, Perry A, Cowdrey C, Croul S, Zadeh G, Korbel JO, Doz F, Delattre O, Bader GD, McCabe MG, Collins VP, Kieran MW, Cho YJ, Pomeroy SL, Witt O, Brors B, Taylor MD, Schüller U, Korshunov A, Eils R, Wechsler-Reya RJ, Lichter P, Pfister SM; ICGC PedBrain Tumor Project: Genome sequencing of SHH medulloblastoma predicts genotype-related response to smoothened inhibition. Cancer Cell *25*: 393-405, 2014.

14 Im S, Choi HJ, Yoo C, Jung JH, Jeon YW, Suh YJ and Kang CS: Hedgehog related protein expression in breast cancer: gli-2 is associated with poor overall survival. Korean J Pathol *47*: 116-23, 2013.

15 Sheng T, Li C, Zhang X, Chi S, He N, Chen K, McCormick F, Gatalica Z and Xie J: Activation of the hedgehog pathway in advanced prostate cancer. Mol Cancer *3*: 29, 2004.

16 Mimeault M and Batra SK: Potential applications of curcumin and its novel synthetic analogs and nanotechnology-based formulations in cancer prevention and therapy. Chin Med *6*: 31, 2011.

17 McKee CM, Xu D, Cao Y, Kabraji S, Allen D, Kersemans V, Beech J, Smart S, Hamdy F, Ishkanian A, Sykes J, Pintile M, Milosevic M, van der Kwast T, Zafarana G, Ramnarine VR, Jurisica I, Mallof C, Lam W, Bristow RG and Muschel RJ: Protease nexin 1 inhibits hedgehog signaling in prostate adenocarcinoma: J Clin Invest *122*: 4025-4036, 2012.

18 Saze Z, Terashima M, Kogure M, Ohsuka F, Suzuki H, Gotoh M: Activation of the sonic hedgehog pathway and its prognostic impact in patients with gastric cancer. Dig Surg *29*: 115-123, 2012.

19 Lee MJ, Hatton BA, Villavicencio EH, Khanna PC, Friedman SD, Ditzler S, Pullar B, Robison K, White KF, Tunkey C, LeBlanc M, Randolph-Habecker J, Knoblaugh SE, Hansen S, Richards A, Wainwright BJ, McGovern K and Olson JM: Hedgehog pathway inhibitor saridegib (IPI-926) increases lifespan in a mouse medulloblastoma model. Proc Natl Acad Sci USA *109*: 7859-7864, 2012.

20 El-Zaatari M, Kao JY, Tessier A, Bai L, Hayes MM, Fontaine C, Eaton KA and Merchant JL: Gli1 deletion prevents Helicobacter-induced gastric metaplasia and expansion of myeloid cell subsets. PLoS One *8*: e58935. 2013.

21 Kasai K, Inaguma S, Yoneyama A, Yoshikawa K and Ikeda H: SCL/TAL1 interrupting locus derepresses GLI1 from the negative control of suppressor-of-fused in pancreatic cancer cell. Cancer Res *68*: 7723-7729, 2008.

22 Quint K, Stintzing S, Alinger B, Hauser-Kronberger C, Dietze O, Gahr S, Hahn EG, Ocker M and Neureiter D: The expression pattern of PDX-1, SHH, Patched and Gli-1 is associated with pathological and clinical features in human pancreatic cancer. Pancreatology *9*: 116-126, 2009.

23 Kelleher FC: Hedgehog signaling and therapeutics in pancreatic cancer. Carcinogenesis *32*: 445-451, 2011.

24 Dai J, Ai K, Du Y and Chen G: Sonic hedgehog expression correlates with distant metastasis in pancreatic adenocarcinoma. Pancreas *40*: 233-236, 2011.

25 Dormoy V, Danilin S, Lindner V, Thomas L, Rothhut S, Coquard C, Helwig JJ, Jacqmin D, Lang H and Massfelder T: The sonic hedgehog signaling pathway is reactivated in human renal cell carcinoma and plays orchestral role in tumor growth. Mol Cancer *8*: 123, 2009.

26 Kim EJ, Sahai V, Abel EV, Griffith KA, Greenson JK, Takebe N, Khan GN, Blau JL, Balis UG, Craig R, Zalupski MM and Simeone DM: Pilot Clinical Trial of Hedgehog Pathway Inhibitor GDC-0449 (Vismodegib) in Combination with Gemcitabine in Patients with Metastatic Pancreatic Adenocarcinoma. Clin Cancer Res pii: clincanres.1269.2014, in press.

27 O'Reilly KE, de Miera EV, Segura MF, Friedman E, Poliseno L, Han SW, Zhong J, Zavadil J, Pavlick A, Hernando E and Osman I: Hedgehog pathway blockade inhibits melanoma cell growth *in vitro* and *in vivo*. Pharmaceuticals (Basel) *6*: 1429-1450, 2013.

28 Riedlinger D, Bahra M, Boas-Knoop S, Lippert S, Bradtmöller M, Guse K, Seehofer D, Bova R, Sauer IM, Neuhaus P, Koch A and Kamphues C: Hedgehog pathway as a potential treatment target in human cholangiocarcinoma. J Hepatobiliary Pancreat Sci *21*: 607-615, 2014.

29 Faria CC, Golbourn B, Dubuc AM, Remke M, Diaz RJ, Agnihotri S, Luck A, Sabha N, Olsen S, Wu X,Garzia L, Ramaswamy V, Mack SC, Wang X, Leadley M, Reynaud D, Ermini L, Post M, Northcott PA, Pfister SM, Croul S, Kool M, Korshunov A, Smith CA, Taylor MD and Rutka JT: Foretinib is effective therapy for metastatic sonic hedgehog Medulloblastoma. Cancer Res pii: canres.3629.2013, 2014, in press.

30 Peluso MO, Campbell VT, Harari JA, Tibbitts TT, Proctor JL, Whitebread N, Conley JM, White KF, Kutok JL, Read MA, McGovern K and Faia KL: Impact of the Smoothened inhibitor, IPI-926, on smoothened ciliary localization and Hedgehog pathway activity. PLoS One *9*: e90534, 2014.

31 Brechbiel J, Miller-Moslin K and Adjei AA: Crosstalk between hedgehog and other signaling pathways as a basis for combination therapies in cancer. Cancer Treat Rev *40*: 750-759, 2014.

32 Kugler MC, Joyner AL, Loomis CA and Munger JS: Sonic Hedgehog Signaling in the Lung - from Development to Disease. Am J Respir Cell Mol Biol PMID 65068457 [Epub ahead of print], 2014, in press.

33 Raz G, Allen KE, Kingsley C, Cherni I, Arora S, Watanabe A, Lorenzo CD, Edwards V DK, Sridhar S, Hostetter G and Weiss GJ: Hedgehog signaling pathway molecules and ALDH1A1 expression in early-stage non-small cell lung cancer. Lung Cancer *76*: 191-196, 2012.

34 Savani M, Guo Y, Carbone DP and Csiki I: Sonic hedgehog pathway expression in non-small cell lung cancer. Ther Adv Med Oncol *4*: 225-233, 2012.

35 Hwang J, Kang MH, Yoo YA, Quan YH, Kim HK, Oh SC and Choi YH: The effects of sonic hedgehog signaling pathway components on non-small-cell lung cancer progression and clinical outcome. World J Surg Oncol *12*: 268, 2014.

36 Kim JE, Kim H, Choe JY, Sun P, Jheon S and Chung JH: High expression of Sonic hedgehog signaling proteins is related to the favorable outcome, EGFR mutation, and lepidic predominant subtype in primary lung adenocarcinoma. Ann Surg Oncol Suppl *3*: S570-576, 2013.

37 Lemjabbar-Alaoui H, Dasari V, Sidhu SS, Mengistab A, Finkbeiner W, Gallup M and Basbaum C: Wnt and Hedgehog are critical mediators of cigarette smoke-induced lung cancer. *1*: e93, 2006.

38 Gialmanidis IP, Bravou V, Amanetopoulou SG, Varakis J, Kourea H and Papadaki H: Overexpression of hedgehog pathway molecules and FOXM1 in non-small cell lung carcinomas. Lung Cancer *66*: 64-74, 2009.

39 Wang QL, Xuo CM, Wu XP, Li YX and Bi XJ: Treatment of atypical gastric dysplasia using Yangzheng Xiaoji. Chin J Diffic Compl Case *7*: 38-39, 2009.

40 Zhang SY, Gu CH, Gao XD and Wu YL: A random, double-blindedand multicentre study of chemotherapy assisted Yangzhengxiaoji capsule on treating primary hepatic carcinoma. Chin J Diffic Compl Case *8*: 461-464, 2009.

41 Ye L, Ji K, Frewer N, Ji J and Jiang WG: Impact of Yangzheng Xiaoji on the adhesion and migration of human cancer cells: the role of the AKT signalling pathway. Anticancer Res *32*: 2537-2543, 2012.

42 Jiang WG, Ye L, Ji K, Ruge F, Wu Y, Gao Y, Ji JF and Mason MD: Anti-tumour effects of Yangzheng Xiaoji in human osteosarcoma, the pivotal role of adhesion kinase (FAK) signalling. Oncol Rep *30*: 1405-1413, 2013.

43 Ye L, Ji K, Ji JF and Jiang WG: Application of Electric Cell-Substrate Impedance Sensing in evaluation of traditional medicine on the cellular functions of gastric and colorecctal cancer cells. Cancer Metastasis Biol Treat *17*: 195-202, 2012.

44 Keese CR, Wegener J, Walker SR and Giaever I: Electrical wound-healing assay for cells *in vitro*. Proc Natl Acad Sci USA *101*: 1554-1559, 2004.

45 Jiang WG, Martin TA, Lewis-Russell JM, Douglas-Jones A, Ye L and Mansel RE: Eplin-alpha expression in human breast cancer, the impact on cellular migration and clinical outcome. Mol Cancer *7*: 71, 2008.
46 Jiang WG, Grimshaw D, Martin TA, Davies G, Parr C, Watkins G, Lane J, Abounader R, Laterra J and Mansel RE: Reduction of stromal fibroblast-induced mammary tumor growth, by retroviral ribozyme transgenes to hepatocyte growth factor/scatter factor and its receptor, c-MET. Clin Cancer Res *9*: 4274-4281, 2003.
47 Martin TA, Parr C, Davies G, Watkins G, Lane J, Matsumoto K, Nakamura T, Mansel RE and Jiang WG: Growth and angiogenesis of human breast cancer in a nude mouse tumour model is reduced by NK4, a HGF/SF antagonist. Carcinogenesis *24*: 1317-1323, 2003.
48 Davies G, Mason MD, Martin TA, Parr C, Watkins G, Lane J, Matsumoto K, Nakamura T and Jiang WG: The HGF/SF antagonist NK4 reverses fibroblast- and HGF-induced prostate tumor growth and angiogenesis *in vivo*. Int J Cancer *106*: 348-354, 2003.
49 Vestergaard J, Pedersen MW, Pedersen N, Ensinger C, Tümer Z, Tommerup N, Poulsen HS and Larsen LA: Hedgehog signaling in small-cell lung cancer: frequent *in vivo* but a rare event *in vitro*. Lung Cancer *52*: 281-290, 2006.
50 Chi S, Huang S, Li C, Zhang X, He N, Bhutani MS, Jones D, Castro CY, Logrono R, Haque A, Zwischenberger J, Tyring SK, Zhang H and Xie J: Activation of the hedgehog pathway in a subset of lung cancers. Cancer Lett *244*: 53-60, 2006.
51 Watkins DN, Berman DM, Burkholder SG, Wang B, Beachy PA and Baylin SB: Hedgehog signalling within airway epithelial progenitors and in small-celllung cancer. Nature *422*: 313-317, 2003.
52 Sims-Mourtada J, Yang D, Tworowska I, Larson R, Smith D, Tsao N, Opdenaker L, Mourtada F and Woodward W: Detection of canonical hedgehog signaling in breast cancer by 131-iodine-labeled derivatives of the sonic hedgehog protein. Biomed Biotechnol *2012*: 639562, 2012.
53 Zahreddine HA, Culjkovic-Kraljacic B, Assouline S, Gendron P, Romeo AA, Morris SJ, Cormack G, Jaquith JB, Cerchietti L, Cocolakis E, Amri A, Bergeron J, Leber B, Becker MW, Pei S, Jordan CT, Miller WH and Borden KL: The sonic hedgehog factor GLI1 imparts drug resistance through inducible glucuronidation. Nature *511*: 90-93, 2014.
54 Castellone MD, Laukkanen MO, Teramoto H, Bellelli R, Alì G, Fontanini G, Santoro M and Gutkind JS: Cross talk between the bombesin neuropeptide receptor and Sonic hedgehog pathways in small cell lung carcinoma. Oncogene doi: 10.1038/onc.2014.104. [Epub ahead of print], 2014, in press.
55 Maitah MY, Ali S, Ahmad A, Gadgeel S and Sarkar FH: Up-regulation of sonic hedgehog contributes to TGF-β1-induced epithelial to mesenchymal transition in NSCLC cells. PLoS *6*: e16068, 2011.
56 Bermudez O, Hennen E, Koch I, Lindner M and Eickelberg O: Gli1 mediates lung cancer cell proliferation and Sonic Hedgehog-dependent mesenchymal cell activation. PLoS One *8*: e63226, 2013.
57 Drenkhahn SK, Jackson GA, Slusarz A, Starkey NJ and Lubahn DB: Inhibition of hedgehog/Gli signaling by botanicals: a review of compounds with potential hedgehog pathway inhibitory activities. Curr Cancer Drug Targets *13*: 580-595, 2013.

Received November 16, 2014
Revised November 25, 2014
Accepted December 2, 2014